

Steps toward dielectronic recombination of argon-like ions: A revisited theoretical investigation of Sc^{3+} and Ti^{4+}

D. Nikolić^a, T.W. Gorczyca^{a,*}, J. Fu^a, D.W. Savin^b, N.R. Badnell^c

^a Department of Physics, Western Michigan University, 1120 Everett Tower, 1903 W. Michigan Avenue, Kalamazoo, MI 49008, United States

^b Columbia Astrophysics Laboratory, Columbia University, New York, NY 10027, United States

^c Department of Physics and Astronomy, University of Strathclyde, Glasgow G4 0NG, United Kingdom

Available online 18 April 2007

Abstract

As an improvement to an earlier study [T.W. Gorczyca, M.S. Pindzola, F. Robicheaux, N.R. Badnell, Phys. Rev. A 56 (1997) 4742], we have calculated dielectronic recombination rate coefficient spectra for Sc^{3+} and Ti^{4+} ions as a test case toward the assembly of a database [<http://homepages.wmich.edu/~gorczyca/drdata/>] for the Ar-like isoelectronic sequence required for modeling of dynamic finite-density plasmas [N.R. Badnell et al., A&A 406 (2003) 1151]. Our theoretical spectra contain dominant $\Delta N = 0$ and $\Delta N = 1$ core excitations channels and exhibit nearly all features found in a recent ion storage ring experiments [S. Schippers, T. Bartsch, C. Brandau, G. Gwinner, J. Linkemann, A. Müller, A.A. Saghir, A. Wolf, J. Phys. B 31 (1998) 4873; S. Schippers et al., Phys. Rev. A 65 (2002) 042723]. In order to compare Maxwellian-averaged rate coefficients, which are of main interest to the astrophysics community, we have developed an iterative deconvolution procedure that enables us to extract the cross-section from storage ring data. After folding the resultant cross-section with a Maxwellian electron velocity distribution, theoretical and experimental rate coefficient spectra agree better than $\sim 18\%$ subject to field reionization effects via high Rydberg states in Sc^{2+} and Ti^{3+} ions.

© 2007 Elsevier B.V. All rights reserved.

PACS: 31.10.+z; 32.80.Dz; 34.80.Lx

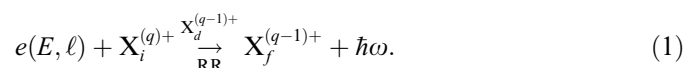
Keywords: Dielectronic recombination; Doubly-excited states in external fields; Merged beams

1. Introduction

The magnetically confining electron-cooled heavy-ion storage rings deliver low divergence high-quality beams of ions for studies of electron–ion collisions. A recent measurement [5] of the electron–ion recombination rate coefficient for Fe^{13+} have indicated the need for improved data in the temperature range where these ions form in photo-ionized plasmas. Following these suggestions and benchmark calculations [6,7] for iron ions with partially filled M shells, this work aims to address electron–ion recombination of Ar-like ions. We first focus on Sc^{3+} and Ti^{4+}

for which preliminary calculations and detailed storage ring experiments are available [1,3,4].

When an incident electron (of kinetic energy E and angular momentum ℓ) is captured by a target ion $\text{X}_i^{(q)+}$ (here X stands for Sc^{3+} or Ti^{4+} initially in the ground state $i \equiv 3s^23p^6$ and we assume a frozen Ne-like $1s^22s^22p^6$ core), an intermediate, doubly-excited resonance state $\text{X}_d^{(q-1)+}$ is formed which can then decay via the emission of a photon to form a bound state $f \equiv 3s^23p^6n'\ell'$, thus completing the process of dielectronic recombination (DR):



We note at this point that the resonant DR pathway competes coherently with the non-resonant, direct pathway of radiative recombination (RR). Calculations of the

* Corresponding author. Tel.: +1 269 387 4913; fax: +1 269 387 4939.
E-mail address: Thomas.Gorczyca@wmich.edu (T.W. Gorczyca).

recombination cross-sections in Eq. (1) often assume that no collisional transitions take place and that no external fields are present.

2. Theoretical calculations and comparison with the experiments

To perform calculations of the DR cross-sections, we employ the multiconfiguration Breit–Pauli (MCBP) atomic structure and collision code Autostructure [8]. This method, which is described more fully in recent works [2,9], includes relativistic and configuration–interaction effects within the independent-processes, isolated resonances, distorted-wave (IPIRDW) approximation (channel coupling and DR + RR interference are neglected). The justification and validity of this approach is discussed in [10] and its merits to modeling of dynamic finite-density plasmas are outlined in [2].

A new development in this code is the use of non-orthogonal one-electron radial functions, generated from a Slater-type orbital (STO) model potential [11] and optimized by varying radial scaling parameters λ_{nl} to minimize the equally weighted sum of eigenenergies belonging to the 17 lowest $3s^2 3p^5 \{3p, 3d, 4s\}$ target levels and the dominant $3p^6 \rightarrow 3p^5 3d$ line strength in the $\text{Sc}^{3+}/\text{Ti}^{4+}$ target ions [12]. By adding bound $n'\ell'$ ($n' \geq 3$) or continuum $E\ell$ orbital to the $3s^2 3p^5 \{3p, 3d, 4s\}$ target configurations, we construct all possible $\text{Sc}^{2+}/\text{Ti}^{3+}$ configurations and use them to evaluate the corresponding configuration-mixed energy levels E_J , Auger rates A^a and radiative rates A^r . Within this framework, partial DR cross-section contributions $\sigma_{i \rightarrow f}^d(\varepsilon)$ of each resonance d in Eq. (1) are given by energy-normalized Lorentzian profiles $L(E, E_d, \Gamma_d)$ of position and width E_d and Γ_d , respectively, with integrated strength:

$$S_{i \rightarrow f}^d = (C_0/\tilde{E}) \times (g_d/2g_i) \times \left(\sum_{\ell} A_{d \rightarrow i, \tilde{E}\ell}^a \right) \times \left(A_{d \rightarrow f}^r \left(\sum_{m, \ell} A_{d \rightarrow m, \tilde{E}\ell}^a + \sum_s A_{d \rightarrow s}^r \right)^{-1} \right), \quad (2)$$

where $C_0 = (2\pi a_0 I_H)^2 \tau_0$, \tilde{E} is the energy of continuum (in Rydbergs), $g_{d,i}$ are statistical weights and $A^{r,a}$ are the radiative/Auger rates in s^{-1} . The third factor in Eq. (2) corresponds to the resonant capture rate and the last factor is the branching ratio for the radiative decay of the resonance state d into the bound state f (versus autoionization). The sum over m accounts for resonant scattering (excitation) and gives the total autoionization width Γ_d^a , whereas s goes over all bound states giving the total radiative width Γ_d^r which may incorporate cascade through autoionizing levels.

The total DR cross-section is obtained by summing the partial cross-sections $\sigma_{i \rightarrow f}^d(\varepsilon)$ over all relevant resonant and final states d and f . For comparison with storage ring experiments [3,4], the sum over final f states is truncated by a “hard cut-off” n'_{cut} (the minimum principal quantum

number of the Rydberg electrons that are reionized due to the motional Stark effect). To find an estimate of the survival probability $P_S(n')$ for certain groups of final states (identified by n'), we use an approach similar to that found in [13]; a comprehensive investigation of the external fields effects based on the specifics of experimental set-up can be found instead in [14]. By convoluting the total DR cross-section $\sigma_i(\varepsilon)$ with a “flattened” Maxwellian electron velocity distribution [15], we obtained the theoretical rate coefficient $\alpha_i(\varepsilon)$. In addition, we use a newly developed iter-

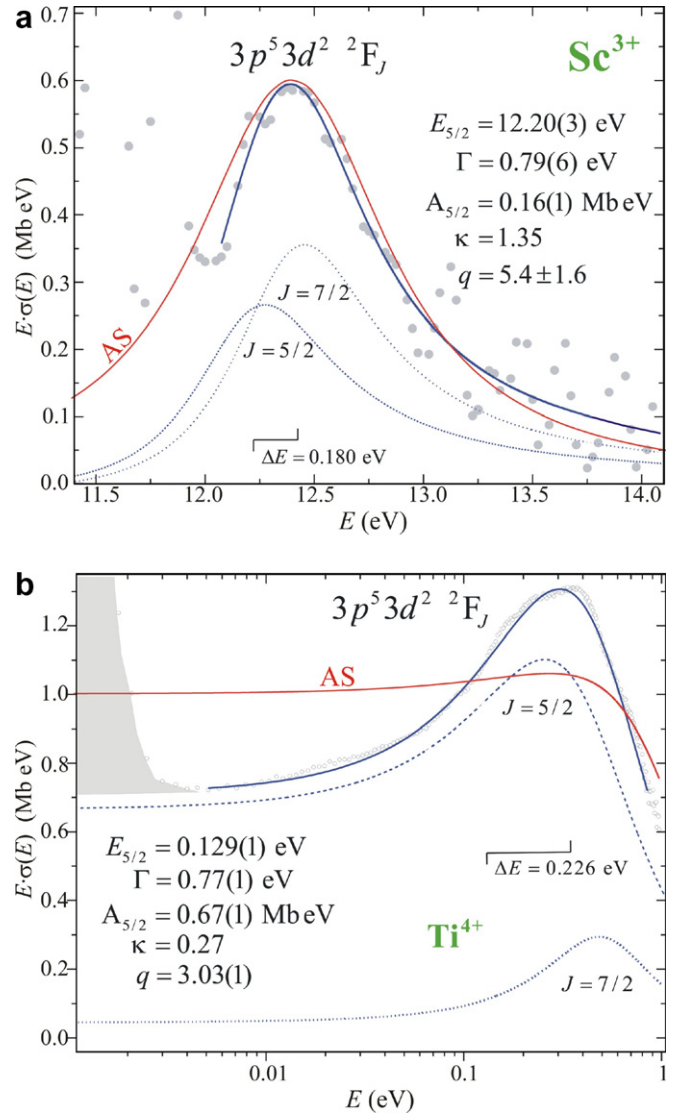


Fig. 1. Modeling of the resonant part of the experimental DR spectra in the vicinity of the 2F_J resonances. Solid (AS) red curve in both cases ((a) for Sc^{3+} and (b) for Ti^{4+}) represents the relevant part of our computed spectra and the solid blue curve is the best fit of the experiment (gray data points) to Eq. (3). Each 2F_J Fano profile is illustrated as blue dotted curve. The fine structure splitting $\delta E = E_{7/2} - E_{5/2}$ was fixed during the fit and $\kappa = A_{7/2}/A_{5/2}$ has been allowed to vary in the final stage of optimization. The shaded area below 4 meV is an unexplained enhancement that is present even in the spectra of bare ions [3]. (For interpretation of the references to color in this figure legend, the reader is referred to the web version of this article.)

ative deconvolution procedure (based on the RATECO-EFF package [16]) to extract a cross-section from the experimental rate coefficient; this allows us to investigate the more subtle features of DR + RR interference, which are manifested most clearly in the asymmetry of the broad $3s^2 3p^5 3d^{22}F$ resonance state [1]. In the absence of interference effects, this resonance profile is given by a Lorentzian profile. However, by taking interference into account, the resonance shape is instead given by a Fano profile [17,18] and can be expressed as [4]:

$$F(E) = \sum_{J=5/2}^{7/5} \frac{4A_J}{\pi\Gamma_J q_J^2} \left[\frac{(q_J + \varepsilon_J)^2}{1 + \varepsilon_J^2} - 1 \right], \quad (3)$$

where we have modeled each of the fine structure components of the resonance separately with differing energy positions $\varepsilon_J = 2E - E_J/\Gamma_J$ and strengths $S_J = 2A_J(1 - 1/q_J^2)$ but with the same asymmetry parameter $q_J = q$ and total width $\Gamma_J = \Gamma$ (see Fig. 1). It is important to note that the position of the maximum in each J -resolved profile is no longer E_J as it is for a Lorentzian profile but is instead shifted to $E_J + \Gamma/2q$. We note that the fitting of our Fano q -parameters is simplified by first constraining the full widths Γ and fine structure splitting $\delta E = E_{7/2} - E_{5/2}$ from Smith's time delay matrix [19]. Our determination of the strengths S_J for Ti^{4+} are in very good agreement with recent measurements of vacuum spark spectra [20] and with atomic structure calculations [21]. For the case of Sc^{3+} , we had to shift our computed $3s^2 3p^5 3d^{22}F$ resonance position by 3.95 eV to lower energies to match the experimental results, whereas for the case of Ti^{4+} no shifting is performed. Also our computed

$3s^2 3p^5 3d^2 {}^2F_J$ resonance widths are larger than those determined by fit of Eq. (3) to experiment. However, for the rest of the recombination spectra (up to 45 eV for Sc^{3+} , see Fig. 2) there are no noticeable interference effects. Therefore, the IPIRDW approximation is still essentially valid for computing total rate coefficients since the 85% of this value is due to contributions from resonances in the 35–43 eV region. More importantly, this energy region is strongly influenced by motional Stark effect through reionization of the recombined $Sc^{2+} 3s^2 3p^6 n' \ell'$ Rydberg states. This is illustrated in Fig. 2, where the upper inset shows predictions of a simple model [13] for survival probability $P_S(n')$ of the $3s^2 3p^6 n' \ell'$ states and suggests the ‘‘hard cut-off’’ $n'_{\text{cut}} = 21$ of [4]. Motional Stark effect plays an important role above 40.5 eV (see Fig. 2) and our calculated rate coefficient has to be modified in accordance to $P_S(n')$ in order to match the experiment.

3. Concluding remarks

We have presented a new computational study of the dielectronic recombination of Sc^{3+} and Ti^{4+} ions and compared these theoretical results to the experimental cross-sections. The newly developed deconvolution procedure gave us a closer insight into experimental recombination cross-sections, where we have confirmed the existence of interference effects between radiative and dielectronic recombination channels, especially in the low energy part of the Ti^{4+} rate coefficient spectra. An overall good agreement with recent merged beams experiments is achieved by modeling of the survival probabilities of high Rydberg states in recombined ions.

Acknowledgements

This work was supported in part by NASA APRA and SHP SR&T programs. D.N. would like to thank S. Schippers for supplying the experimental results in numerical form.

References

- [1] T.W. Gorczyca, M.S. Pindzola, F. Robicheaux, N.R. Badnell, Phys. Rev. A 56 (1997) 4742.
- [2] N.R. Badnell et al., A&A 406 (2003) 151.
- [3] S. Schippers, T. Bartsch, C. Brandau, G. Gwinner, J. Linkemann, A. Müller, A.A. Saghiri, A. Wolf, J. Phys. B 31 (1998) 4873.
- [4] S. Schippers et al., Phys. Rev. A 65 (2002) 042723.
- [5] E.W. Schmidt et al., Astrophys. J. 641 (2006) L157.
- [6] N.R. Badnell, J. Phys. B 39 (2006) 4825.
- [7] N.R. Badnell, Astrophys. J. 651 (2006) L73.
- [8] N.R. Badnell, J. Phys. B 19 (1986) 3827.
- [9] N.R. Badnell, J. Phys. B 30 (1997) 1.
- [10] M.S. Pindzola, N.R. Badnell, D.C. Griffin, Phys. Rev. A 46 (1992) 5725.
- [11] A. Burgess, H.E. Mason, J.A. Tully, A&A 217 (1989) 319.
- [12] <http://physics.nist.gov/PhysRefData/ASD/index.html>.
- [13] T. Mohamed, D. Nikolić, E. Lindroth, S. Madzunkov, M. Fogle, M. Tokman, R. Schuch, Phys. Rev. A 66 (2002) 022719.

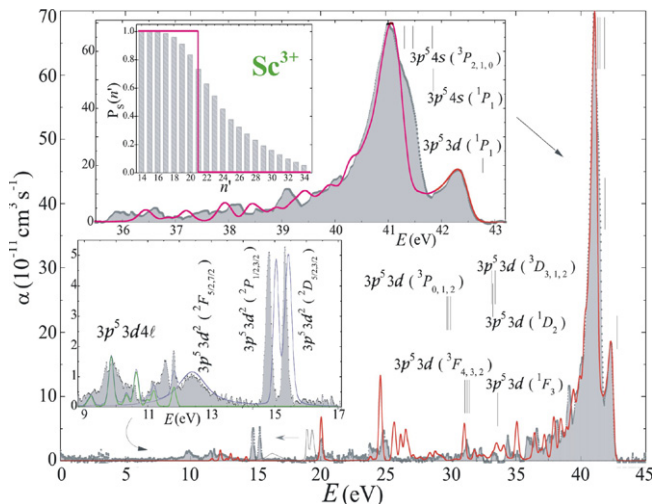


Fig. 2. Calculated (red curve) and measured (shaded area) DR rate coefficients for Sc^{3+} . The upper inset enlarges the spectra of the Rydberg series converging to the four highest thresholds including the modeling of motional electric field effects. The lower inset shows the spectra in the vicinity of the broad and asymmetric $3p^5 3d^2 {}^2F$ resonance. The theoretical results are shifted by -3.95 eV and -2.45 eV for the $3p^5 3d^2$ and $3p^5 3d 4s$ resonances, respectively. (For interpretation of the references to color in this figure legend, the reader is referred to the web version of this article.)

- [14] S. Schippers, A. Müller, G. Gwinner, J. Linkemann, A.A. Saghiri, A. Wolf, *Astrophys. J.* 555 (2001) 1027.
- [15] P.F. Dittner, S. Datz, P.D. Miller, P.L. Pepmiller, *Phys. Rev. A* 33 (1986) 124.
- [16] D. Nikolić, Licentiate Thesis, University of Stockholm, 2003.
- [17] U. Fano, *Phys. Rev.* 124 (1961) 1866.
- [18] U. Fano, J.W. Cooper, *Phys. Rev.* 137 (1965) A1364.
- [19] F.T. Smith, *Phys. Rev.* 118 (1960) 349.
- [20] A.N. Ryabtsev, S.S. Churilov, É.Ya. Kononov, *Opt. Spectrosc. B* 98 (2005) 519.
- [21] A.E. Kingston, A. Hibbert, *J. Phys. B* 39 (2006) 2217.